Regulation of endothelial DNA methylation by the sustained response to IL-6

Ramon Bossardi Ramos[1*], Nina Martino[1], Dareen Chuy[1], Shuhan Lu[1], Alejandro P. Adam[1,2*].

Affiliations:

[1]Department of Molecular and Cellular Physiology, Albany Medical Center, Albany, New York.

[2]Department of Ophthalmology, Albany Medical Center, Albany, New York.

*Address all correspondence to:

Alejandro P Adam, PhD, adama1@amc.edu

Ramon Bossardi Ramos, PhD, bosarr@amc.edu

Albany Medical College. 43 New Scotland Avenue, Albany, NY 12208. Tel: 518.262.3140

Conflicts of Interest: The authors declare no conflicts of interest.

Abstract

Interleukin 6 (IL-6) is a major mediator of the cytokine storm during shock. Its actions on the endothelium lead to pathological vascular leakage, leukocyte adhesion, and coagulopathy, which may result in multiorgan dysfunction and potentially death. Many shock survivors suffer long-term sequelae. We hypothesize that shock-induced endothelial epigenetic changes are involved in orchestrating these chronic pathological changes. Here, we interrogated the DNA methylation changes in the kidney endothelium after a challenge with lipopolysaccharides (LPS) in wilt type (WT) mice and in mice lacking endothelial SOCS3 ($SOCS3^{iEKO}$). We identified 2596 differentially methylated positions (DMP) after an LPS challenge in WT mice. Notably, lack of endothelial SOCS3 leads to a highly divergent response, with 3564 DMP in response to LPS in $SOCS3^{iEKO}$ vs WT mice. Consistent with the hyper-inflammatory response in $SOCS3^{iEKO}$ mice, gene ontology analysis shows an enrichment in genes associated with an inflammatory response. To assess whether endothelial cells respond to IL-6 signaling directly by inducing DNA methylation changes, we challenged human umbilical vein endothelial cells in culture with IL-6 for 72 hours prior to methylomics assays. DNA methylation modifications were observed in sites associated with pathways regulating the regulation of cell adhesion, proliferation, and cytokine signaling. To determine the stability of these changes, we treated cells with IL-6 for 72h, followed by 96h in the absence of IL-6. We found that 40% of the DMP remained modified after the cytokine wash with a mean difference of less than 2% when comparing washed (72+96h) vs. non-washed cells (72h alone), suggesting that many changes in the endothelial methylome may remain in place for prolonged periods. In summary, persistent activation of endothelial IL-6 signaling leads to endothelial DNA methylation changes. Together, our data demonstrate that in response to pro-inflammatory stimuli, the endothelium elicits epigenetic changes that are at least in part due to IL-6/STAT3/SOCS3 signaling. These changes may regulate pathways associated with reduced long-term survival and chronic organ damage after shock.

Introduction

Severe shock is a dysregulated host response to infection, burn, or trauma, eventually inducing vascular dysfunction and leading to multiorgan failure and death. Septic shock is one of leading cause of death among hospitalized patients[1]. Shock affects practically all aspects of endothelial function, including increases in vascular leak, leukocyte adhesion, and thrombosis[2]. This endothelial dysfunction is thought to be a critical factor in the progression from septic shock to organ failure[3]. Despite advances in intensive care, septic shock survivors may experience long-term sequelae, including chronic cardiovascular and kidney dysfunction, cognition impairment, and mental health issues, a syndrome known as PICS[4]. However, the mechanisms driving PICS are not understood. Over the last years, extensive efforts have been made to define the role of epigenetic regulation, including DNA methylation, in sepsis. Substantial DNA methylation modifications in circulating cells occur in septic patients[5-7], which has been suggested to contribute to immune activation and tolerance[8, 9]. It is conceivable that similar epigenetic changes occur within the affected organs, but limitations in the availability of septic samples greatly restricts our understanding beyond circulating cells. In particular, the precise endothelial epigenetic changes and their potential impact in the long-term effects of shock are not known. Understanding these changes may provide a potential avenue to understand the link between abnormal gene expression and chronic inflammation after the initial shock subsided.

The levels of many cytokines are dramatically altered during a cytokine storm, but the circulating levels of IL-6 are particularly informative as they correlate with systemic disease severity[10, 11] and are highly predictive of mortality[12]. Over time, an IL-6 amplifier mechanism that consists of a positive feedback regulation of this cytokine has been linked to a worse prognosis[11]. These defects are mediated mainly by excessive IL-6 trans-signaling[13], which involves binding to a circulating, soluble form of the alpha subunit of the IL-6 receptor (sIL6Rα) to induce STAT3 phosphorylation via gp130 and JAK kinases. The pathway is inhibited by a negative feedback loop involving de novo synthesis of SOCS3[14, 15]. Previous work from our lab demonstrated that IL-6 signaling promotes STAT3-dependent sustained barrier function loss in human endothelial cells (EC) primary cultures, both directly[16] and as an autocrine loop induced by endotoxin (lipopolysaccharides from *E Coli*, LPS) or TNF[17]. Further, we recently showed that loss of SOCS3 in the endothelium leads to fast mortality after an endotoxemic challenge that is not lethal in wild type (WT) mice, which is preceded by severe vasculopathy and kidney failure[18], demonstrating the critical role for this pathway within the endothelium of mice under severe systemic inflammation and providing a potential mechanism for shock-induced vasculopathy.

Here, we sought to determine the role of the IL-6/STAT3/SOCS3 signaling axis in the regulation of the endothelial DNA methylation changes in response to pro-inflammatory stimuli. We found that a single endotoxin challenge leads to substantial DNA methylation changes in the kidney endothelium. Moreover, lack of endothelial SOCS3 dramatically alters the kidney endothelium DNA methylation landscape. Gene ontology analysis showed an enrichment of genes involved in inflammation, cytokine signaling, and leukocyte adhesion, suggesting that the acute inflammatory response may lead to long-lasting changes in endothelial inflammation. In vitro, we demonstrate that IL-6 induces changes in DNA methylation, and many changes in the endothelial methylome may remain in place for prolonged periods even without IL-6 sustained signaling. Together, these findings demonstrate that the endothelium responds to shock with changes in DNA methylation and show a potential role for IL-6 signaling and its inhibitor SOCS3 as key regulators of the inflammation-induced epigenetic changes.

Materials and methods

Materials

The commercial sources for critical reagents and their catalog numbers are listed in Supplemental Table 1. Supplemental Table 2 provides a list of sequences for RT-qPCR primers. Supplemental Table 3 lists all antibodies used.

Mice

Mice were housed in specific pathogen-free rooms with 12-hour light/12-hour dark cycle and controlled temperature and humidity. Mice were kept in groups of 5 or fewer in Allentown cages with access to food and water ad libitum. Endothelial-specific, tamoxifen-inducible SOCS3 knockout ($SOCS3^{iEKO}$) mice on a C57Bl6/J background were described previously[18]. Briefly, all mice carried two copies of a Cdh5-CreERT2 endothelial driver[19] and ROSA26-tdTomato reporter[20] by crossing B6.Tg(Cdh5-cre/ERT2)1Rha with B6.Gt(ROSA)26Sor$^{tm9(CAG\text{-}tdTomato)Hze}$. A floxed SOCS3 transgene[21] was introduced by breeding to B6;129S4-Socs3^{tm1Ayos}/J to generate the $SOCS3^{iEKO}$. Control and $SOCS3^{iEKO}$ littermates were obtained by breeding two $SOCS3^{fl/+}$ heterozygous mice. Genotyping primers have been described previously[18]. All mice received tamoxifen (2 mg tamoxifen in 100 µL via intraperitoneal (IP) injection) at 6–9 weeks old for 5 consecutive days. All the experiments were conducted between 2 and 3 weeks after the end of tamoxifen treatment and SOCS3 deletion gene was confirmed by post-tamoxifen tail digestion and PCR.

Severe, acute inflammation was induced by a single IP injection of a bolus of 250 µg/250 µl LPS. Control mice were given 250 µl of sterile saline via IP injection. Disease severity was scored 14 hours after the LPS challenge as described before[18]. Immediately after scoring, body weight and temperature were measured. Mice were then euthanized with an overdose of pentobarbital. No mice were excluded from the studies. Assignment to the saline or LPS groups was performed through randomization of mice within each genotype and sex for each litter. All handling, measurements, and scoring were performed by a researcher masked to treatment and genotype groups and based on mouse ID (ear tags). Experimental groups were unmasked at the end of each experiment.

Enrichment of endothelial cells for DNA methylation studies

After euthanasia, the animals were cannulated on the left ventricle, and the right atrium was nicked to allow perfusion with 5 ml/min PBS for 3 min. Kidneys were collected and minced into small pieces (~1 mm^3). The tissues were transferred to 50 ml conical tubes containing 5 ml of PBS containing calcium and magnesium plus 100 mg of type 1 collagenase and 100 mg dispase II for 10 minutes at 37°C. The slurry of tissue and buffer was triturated by passage through a 14-gauge cannula attached to a 10 ml syringe approximately 10 times, followed by a 20-gauge cannula attached to a 10 ml syringe. The cell suspensions were filtered through a 70 µm cell strainer, resulting in single cell suspensions prior to centrifugation at 400×g for 8 min at 4 °C. Pellets were resuspended with 1.5ml of ice-cold PBS + 0.1% BSA. One aliquot (75 µl) per sample was lysed in Trizol to obtain whole kidney RNA.

The remaining of cell suspensions were transferred to RNAse free polystyrene tubes containing 60 µl of streptavidin-conjugated dynabeads bound to biotinylated EpCAM and biotinylated CD45 antibodies. The cell suspensions were incubated with these beads for 10 min at RT with rotation. Following this, tubes were placed on a Dynal MPC-S magnet for 5 minutes. The supernatants were transferred to RNAse free polystyrene tubes containing 45ul of streptavidin-conjugated dynabeads bound to biotinylated CD31 antibodies and incubated for 10 min at RT with rotation. Following this, tubes were placed on a Dynal MPC-S magnet for 5 minutes and the supernatant was discarded. The remaining cells bound to the beads were

washed six times with PBS containing 0.1% BSA to remove any contaminating cells. After removal of the final wash, the cells were resuspended in 400 µl PBS. Of these, 200 µl were transferred to an RNAse-free tube and proceeded to DNA isolation using the DNeasy Blood & Tissue Kits (Qiagen, USA). The other 200 µl were used for RNA isolation following the RNeasy Plus Mini Kit (Qiagen) protocol. VWF and CDH1 expression were measured by RT-qPCR. The ratios of VWF and CDH1 expression in the enriched versus the total RNA from the same organ were calculated to confirm the enrichment of the endothelial cells following this protocol.

Cell culture

Human Umbilical Vein Endothelial Cells (HUVECs) were isolated in-house according to established protocols[22-24] as described before[16-18]. The identity and purity of the HUVEC isolations were confirmed for each isolation by more than 99% positive immunostaining with endothelial cell markers (FITC-Ulex europaeus lectin, VE-cadherin) and more than 99.9% negative for α–smooth muscle actin. Cells were assayed between passages 3 and 8. To induce IL-6 signaling, cells were plated at full confluence at a density of 8×10^4 cells/cm^2 on plates precoated for 30 min with 0.1% gelatin and incubated at least 48 h prior to the start of experiments. Cells were then treated with a combination of 200 ng/mL recombinant human IL-6 and 100 ng/mL sIL-6Rα (IL-6+R) or PBS (control) for 72 hours. After 72 hours, a subset of control and IL-6+R-treated cells were washed and incubated for 96 hours in EGM-2 Growth Medium. Treated HUVECs and controls were immediately lysed in Trizol or centrifuged and stored until DNA extraction.

RT-qPCR

Cells grown on multi-well plates were lysed with Trizol reagent (Thermo Fisher), and RNA was extracted with chloroform and precipitated with isopropanol as per manufacturer's instructions. A total of 400 ng of RNA was used to prepare cDNA using Primescript RT Master Mix (Clontech) at 42 °C following manufacturer's instructions. Depending on the target, cDNA was diluted 10-fold in nuclease-free water. Then, 2 µl of cDNA was used per PCR reaction. qPCR was performed in a StepOnePlus (Applied Biosystems) instrument using SYBR green-based iTaq supermix (Bio-Rad) and 2 pmol primers (Thermo Fisher). Fold induction was calculated using the ΔΔCt method using GAPDH (human) or HPRT (mouse) as housekeeping gene.

DNA isolation, bisulfite treatment, and methylation profiling

DNA was isolated using the DNeasy Blood & Tissue Kit (Qiagen, USA) according to the manufacturer's instructions, including optional treatment with 100 mg/ml RNase A. The concentration of DNA was measured by the Qubit dsDNA BR Assay Kit (Molecular Probes). The DNA samples were stored at -80°C. Bisulfite conversion of 500 ng of genomic DNA was performed using an EZ DNA Methylation-Gold™ Kit (Zymo Research) following manufacturer's instructions. Analysis of DNA methylation was carried out using Illumina Infinium MethylationEPIC BeadChip arrays[25] for human genomes (>850K sites) and Infinium Mouse Methylation BeadChip arrays for mouse genomes (>285K sites) by the Epigenomic Services from Diagenode.

DNA methylation data processing

Methylation array data were processed with the statistical language R (version 4.2.1) and Bioconductor packages. Processing of the raw HUVEC methylation data was performed with the Chip Analysis Methylation Pipeline (ChAMP) package (version 2.21.1)[26]. Raw methylation data were imported by the minfi method[27, 28]. Probes with a detection p-value >0.01 in one or more samples, with a bead count <3 in at least 5% of samples, non-CpG probes, probes that align to multiple locations, and sex chromosome-specific probes were removed from

subsequent analyses. As a result, the remaining 727,127 probes were utilized for data analysis. Data normalization was performed by the BMIQ method[29]. Batch effect prediction was made by singular value decomposition (SVD)[26]. Mouse data, probe, and intensity data for each sample were imported into R using the package RnBeads (version 2.10.0)[30], followed by preprocessing to filter probes outside the CpG context, SNP probes, sex chromosome probes, probes without intensity value, and probes with a low standard deviation[27, 31, 32]. The RnBeads.mm10 package was used to annotate the location of each probe. Downstream data analysis was performed using β values. The β value is the ratio of the methylated probe intensity to the overall intensity (the sum of the methylated and unmethylated probe intensities). βvalues range from 0 to 1, in which 0 is no methylation and 1 is complete methylation and were used to derive heatmaps and further analysis[33]. Differential methylation between groups was defined as $\Delta\beta$ value difference and adjusted p-value (Benjamini-Hochberg method, FDR <0.05).

Gene ontology (GO) analysis of the differentially hypomethylated or hypermethylated CpG sites associated with gene locations was performed using Metascape (version 3.5)[34] and selecting GO terms with a p-value less than 0.05. Motif enrichment of the same CpG sets was done using findMotifsGenome.pl program of the HOMER (version 4.11)[35] and selecting a 500-bp window upstream and downstream of the differentially methylated CpG sites. Annotated CpGs in the EPIC array were used as background.

RESULTS

LPS induces altered DNA methylation and transcriptional changes in the kidney endothelium.

To better understand the mechanisms underlying DNA methylation changes associated with the exposure to bacterial endotoxin, we first challenged the mice with a single dose of endotoxin (250 µg/mouse of lipopolysaccharides from E. coli 0111:B4, LPS) or saline solution. As expected, we observed that LPS induced a systemic response, as measured 14 h post-challenge (Figures 1A and 1B). We previously demonstrated that this treatment leads to severe kidney injury[18]. Epigenetic changes are dynamic and tissue-specific[36], and may underly kidney injury and repair[37]. To assay the epigenetic changes occurring in the kidney endothelium, after obtaining single cell suspensions, we enriched endothelial cells using a two-step approach of negative selection of non-endothelial cells using EpCAM- and CD45-labeled magnetic beads, followed by a positive EC selection with PECAM (CD31)-labeled beads (Figure 1C). To ensure EC enrichment, we measured by RT-qPCR the expression levels of CDH1 (an epithelial marker) and VWF (an endothelial marker) in the RNA obtained from the kidney cell suspension before and after magnetic bead enrichment. As shown in Figure 1D, VWF detection was increased, and CDH1 decreased, when comparing EC RNA to total RNA.

We then processed the DNA obtained from the same cell suspensions to detect methylation changes using Infinium Mouse Methylation BeadChip arrays of bisulfite-treated DNA. These arrays allow us to interrogate the DNA methylation status of >285,000 CpG sites across the entire mouse genome. We found that kidney EC from endotoxemic mice displayed 804 CpG sites with significantly lower methylation levels (hypomethylated) and 1792 with significantly higher methylation levels (hypermethylated) than control endothelial cells, with an FDR <0.05 (Figure 1E). We performed gene ontology (GO) analysis to determine whether the differentially methylated genes were associated with relevant biological processes in the inflammatory response. In the hypermethylated set, there was an enrichment in categories such as cell adhesion, regulation of cell junction, and cAMP signaling pathway. In the hypomethylated group, functional categories were also associated with innate immunity, including cytokine signaling, NF-κB signaling regulation, and IL-6 production (Figure 1F).

Inspection of individual genes among those containing differentially methylated CpG sites made it possible to identify some with functions associated with endothelial cell regulation and inflammation (Figure 1G). These included hypermethylated sites within genes such as Pcdha1, a cell adhesion gene from the cadherin superfamily[38], and Thsd4, a thrombospondin associated gene[39], as well as hypomethylated sites in LPP, a LIM domain-containing protein involved in cell-cell adhesion[40] and MAP3K14, coding for NIK, a kinase involved in NF-κB activation[41] and associated with kidney injury through the promotion of inflammation and cell death[42]. All these examples highlight the relationship between the genes undergoing changes on DNA methylation and endothelial cell response to the endotoxin.

Loss of endothelial SOCS3 promotes a divergent response to LPS

Previously, we have shown a dramatic increase in whole-tissue IL-6 mRNA levels in the kidneys after LPS treatment in the WT and a higher increase in the SOCS3^{iEKO} mice[18]. Further, we recently shown that, at least in vitro, an IL-6 autocrine loop mediates severe endothelial dysfunction in response to LPS or TNF[17]. Given the hypomethylation of genes associated with pro-inflammatory NF-κB signaling and IL-6 production, we hypothesized that the endothelium may be an important source of IL-6 in the context of systemic inflammation, explaining at least in part the kidney failure and lethality of SOCS3^{iEKO} in response to LPS[18]. To assess if the increase in whole kidney IL-6 mRNA levels is associated with the endothelium, we measured its expression in kidney EC mRNA enriched as above. RT-qPCR analysis showed that LPS induced a marked increase in EC-specific IL-6 RNA (Figure 2A). Consistent with an activation of an IL-6 amplifier loop in SOCS3^{iEKO} mice, these mice showed an increased response when compared to the LPS. Similar changes were also observed when measuring PTGS2 mRNA levels (Figure 2A), a marker of an inflamed endothelium we have previously shown to be highly dependent on IL-6 signaling[17, 18]. Thus, it is appealing to hypothesize that loss of SOCS3 leads to altered DNA methylation that is a driver of inflammatory response in the endothelium.

We found that 2189 CpG sites were hypomethylated and 1375 were hypermethylated with an FDR < 0.05 when comparing the changes in endotoxemic SOCS3^{iEKO} vs control mice (Figure 2B). GO analysis of hypomethylated CpGs in the LPS/SOCS3^{iEKO} group revealed an enrichment of functional categories associated with endothelial cell biology and inflammation, including regulation of MECP2 expression, regulation of NF-Kappa B signaling, and leukocyte differentiation. In contrast, GO analysis of hypermethylated sites showed an enrichment of regulatory categories such as regulation of transmembrane transport, cell surface signaling, and negative regulation of ERK1 and ERK2 cascades (Figure 2C). Analysis of the tracks of individual genes (Figure 2D) revealed that CpG sites inside the genes Pcdha1 and Hoxc4 are associated with hypomethylation. HOXC4 is an important regulator of transcription in B cell differentiation[43] and promotes NF-κB signaling and proliferation[44]. In the hypermethylation set, C1qtnf1, which codes for complement C1q TNF-related protein 1, promotes endothelial barrier dysfunction[45], while Enpp4 is involved in positive regulation of blood coagulation and purine ribonucleoside catabolic processes[46].

To detect potential transcription factors involved in the regulation of the methylation status of these genes, we performed motif enrichment analysis of the hypermethylated and hypomethylated subsets. Hypermethylated CpGs of LPS-treated endothelial cells in SOCS3^{iEKO} mice were enriched in transcription factor binding motifs relevant to inflammation, such as bZIP family (including AP1 family members JunB, ATF3, and FRA2), and some members of the IRF family (IRF1, IRF2, IRF3). In contrast, hypomethylated CpGs contained motifs for several homeobox family factors. Other binding sites, such as that for CTCF, were present in both groups (Figure 2E). Collectively, these results revealed specific TFs associated with both groups, suggesting a potential mechanism driving gene-specific methylation changes.

Direct IL-6 signaling in vitro promotes sustained DNA methylation and RNA expression changes in HUVEC

Our mouse studies identified epigenetic changes in the injured kidney endothelium that were associated with an increase in IL-6 expression. Moreover, overactivation of this pathway via loss of the negative regulator SOCS3 leads to an altered epigenetics signature with a heightened transcriptional response. To better understand the direct effects of IL-6 signaling in EC DNA methylation, we performed experiments using cultured primary human umbilical vein endothelial cells treated with recombinant IL-6 and soluble IL-6Rα (herein, IL-6+R). Our prior research showed acute transcriptional changes and sustained barrier function loss upon an IL-6+R challenge[16, 18]. Here, we sought to determine whether gene expression was similarly sustained. Our findings showed that 72 hours of sustained IL-6+R treatment resulted in increased levels of SOCS3 mRNA, as well as those of IL-6 itself (Figure 3A). We also found sustained changes in other IL-6-responsive genes, including CXCL2 and RHOU (Figure 3A).

To determine if the changes in gene expression were associated with a differential DNA methylation signature, we extracted DNA from these cells and performed bisulfite conversion. For the analysis, we used Illumina Infinium MethylationEPIC BeadChip arrays to interrogate the methylation status of >850,000 CpG sites across the entire human genome, covering 99% of RefSeq genes. De novo unbiased clustering of the data distinctly segregated HUVEC treated with saline solution from those treated with IL-6+R (Figure 3B). This treatment led to 205 hypomethylated and 226 hypermethylated CpG sites, with an FDR <0.05 (Figure 3B). Of those, approximately 65% were located near the transcription start site or within genes, while the other 35% were located in intergenic regions (Figure 1C). GO analysis of the subset of differentially methylated sites located near or at genes revealed distinct enriched biological processes for hypo- and hypermethylated CpG clusters in relation to IL-6+R treatment, including regulation of cell adhesion, response to cytokine stimulus, and endothelial cell differentiation (Figure 3D).

Given the changes on DNA methylation, we assayed the correlation between DNA methylation changes and gene expression. Inspection of individual genes among those containing differentially methylated CpG sites made it possible to identify some candidate genes with changes in gene expression. These include genes such as LAMP3, a lysosomal-associated membrane protein 3, which is increased during stress response[47], and showed hypomethylation and increased gene expression. The opposite was observed with MYO10, a gene sensitive to inflammatory stimuli[48], and ADAM19, an enzyme from a disintegrin and metalloproteinase family, involved in profibrotic and proinflammatory processes leading to renal deterioration[49], which the hypermethylation in a specific position was associated with decreased gene expression (Figure 3E). Together, these results suggest the changes in methylation observed after IL-6 signaling can impact gene expression.

Changes in methylation patterns are retained after IL-6 signaling interruption.

We then wondered whether the DNA methylation patterns could be maintained and impact the gene expression after IL-6+R signaling ends. To investigate this, HUVEC were incubated for 72 hours with IL-6+R or saline. Then, cells were either lysed or washed and incubated for an additional 24h or 96 h in regular growth media. Under these conditions, we confirmed that IL-6 mRNA expression was highly induced by IL-6+R, but this response was abrogated within 24 h of signal termination (Figure 4A). Consistently, we found that the increased STAT3 phosphorylation induced by an IL-6+R challenge returned quickly back to control levels after the treatment wash, demonstrating complete removal of the cytokine (Figure 4B). Notably, we found that LAMP3 mRNA expression remains increased even 96 h after the IL-6 signaling interruption (Figure 4C), suggesting a potential role for DNA methylation in regulating LAMP3 expression levels. To test this, we measured DNA methylation in cells 96 h after IL-6 washout. Figure 5A

shows that, despite this signal abolition, 39.2% of the methylation changes observed after 72 hours of IL-6+R remained altered post-washout (with a mean difference of less than 2% and FDR ≤ 0.05), suggesting that many changes in the endothelial methylome may remain in place for prolonged periods, potentially inducing long-lasting transcriptional changes. Analysis of transcription factor (TF) motif enrichment using HOMER demonstrates differences in the motif that are overrepresented in the hypo- and hyper-methylated groups. Notably, hypomethylated CpG after IL-6+R treatment were enriched in STAT (in particular STAT1 and STAT3) binding motifs, suggesting that the direct transcriptional regulation may be linked to DNA demethylation (Figure 5B). Similarly, we have previously identified an acute transcriptional response involving the activation of the interferon regulatory factor (IRF) family of transcription factors[18], and here we show that IRF-binding motifs are enriched in the hypermethylated subset (Figure 5B). Other relevant to inflammatory response sites enriched in differentially methylated genes include those bound by ETS, zinc finger (ZF), bZIP, homeobox, and bHLH families (Figure 5B). We then inspected the enrichment of TF binding motifs among 72 hours IL-6+R and 96 hours wash. We observed a significant overrepresentation of a subset of the TF identified upon 72 hours of IL-6+R treatment, including GATA4, GATA6, Nrf2, and HOXC9 in hypomethylated regions, and ATF3, AP1, Bcl6, ZEB1, ASCL2 and BHLH40 in hypermethylated regions. Interestingly, we previously showed[18] that some of these TFs are quickly induced by IL-6+R, including the API members JunB and Fra1, BATF, and Bcl6.

Discussion

Here, we present evidence to support the notion that DNA methylation in endothelial cells is affected by shock, affecting genes potentially involved in inflammation-induced endotheliopathy. Our study suggests a potential role for IL-6 signaling and SOCS3, the main negative regulator of IL-6, as key regulators of inflammation-induced epigenetic changes. Most notably, changes that occur during the IL-6 signaling in cultured human cells are retained after the interruption of the cytokine signaling, suggesting that IL-6 may have long-term effects in the endothelium well after the resolution of inflammation.

Sepsis survivors have increased risk of developing chronic cardiovascular, kidney, and cognitive dysfunction[4]. DNA methylation changes in the endothelium may play a role in the chronic dysfunctions associated with these chronic sequelae. For example, studies have linked DNA methylation with heart failure (HF)[50-52]. EC dysfunction is a critical mechanism in HF pathogenesis[53, 54]. Current published data on DNA methylation modifications in septic patients have been predominantly examined in mixed populations of circulating cells[5, 6]. For example, one study identified 668 methylation sites that were altered between patients with sepsis from those with non-septic critical illness[5]. Indeed, across functional enrichment analysis, DNA methylation alterations have been identified in methyltransferase activity, cell adhesion, and cell junctions[5]. Furthermore, several studies provide evidence suggesting that the expression of enzymes involved in epigenetic modifications and chromatin remodeling varies with sepsis severity and cell type[6, 55, 56]. In addition, an in vitro study using genome-wide DNA methylation status of cultured cells isolated from mouse kidneys identified 200 genes with differentially methylated promoters 24h after ischemia and reperfusion injury, of which 79 maintained the difference 7 days after reperfusion[57]. Another report showed 1,721 genes are differentially methylated in rat lung tissue in response to LPS-induced acute lung injury[58]. The study of DNA methylation in shock animal model is an emerging area[37, 59], but further research is needed, especially in to understand the cell type-specific epigenetic changes. In particular, little is known about the endothelial epigenetic response to shock.

Because the endothelium is a major mediator of organ dysfunction in response to shock[3, 60-64], we hypothesized that epigenetic alterations in the endothelium may lead to sustained organ damage (e.g., lungs, kidneys) via prolonged vascular dysfunction, including systemic vascular

leak, thrombosis, and increased leukocyte adhesion[65]. However, the specific role of the epigenetic changes within the endothelium in failing organs is not well understood. Here, we identified multiple modifications in the DNA methylation on the kidney endothelium in the endotoxemic mice that were associated with an increased inflammatory response. We focused on the kidney because of its well characterized injury in mouse models of systemic inflammation[18, 66] and because we previously showed a dramatic loss of kidney function in endotoxemic SOCS3^{iEKO} mice[18]. Consistently, loss of endothelial SOCS3 led to a differential epigenetic signature in response to LPS than WT mice. A gene ontology analysis showed an enrichment of pathways downstream of inflammatory cytokines and cell adhesion. In addition, we detected changes associated with several TF binding motifs regulating the inflammatory response, as well as endothelial processes such as EC proliferation, junction formation, or arteriovenous differentiation[67].

Accumulating evidence suggests that excessive IL-6 trans-signaling can mediate in large part disseminated intravascular coagulopathy, pathological vascular leakage, and leukostasis[10, 13]. The mechanism involves binding to a circulating, soluble form of the alpha subunit of the IL-6 receptor (sIL6Rα) to induce STAT3 phosphorylation via gp130 and JAK kinases. The pathway is inhibited by a negative feedback loop involving de novo synthesis of SOCS3[10, 11]. We previously shown that IL-6 signaling (directly, or as an autocrine loop induced by LPS or TNF) promotes STAT3-dependent sustained barrier function loss[16-18]. A recent study showed that the changes in DNA methylation in human monocytes from individuals following a septic episode correlate with their circulating IL-10 and IL-6 levels, suggesting a potential mechanism downstream of these cytokines participating in the defective generation of DNA methylation alterations[68]. Notably, this study also showed significant changes in the methylation status of interferon response genes[68]. A second study showed that LPS leads to changes in monocyte DNA methylation that are concomitant with the upregulation of inflammatory-related genes, and these involve the JAK2/STAT pathway[69]. Together, these reports and our findings that IL-6 regulates the expression and methylation of interferon stimulated genes in endothelial cells (reference[18] and this study), suggest that leukocytes and the endothelium may respond with similar transcriptional modules.

Interestingly, our study observed an enrichment in AP-1 binding sites nearby hypermethylated positions 72 hours after an IL-6+R treatment that remained differentially methylated 96 hours after wash. A TF member of the AP-1 family, MaFb[70] is required for angiogenesis through the regulation of small GTPases controlling cytoskeletal dynamics and thereby cell migration[67, 71], which are functions that we observed associated with DMP through the GO analysis. Further, the opposite response (i.e., hypomethylated CpGs in response to IL6+R) was associated with binding sites to the Zinc Finger family TFs GATA4 and GATA6. Modulation of GATA4 levels impacts the expression of genes involved in cytoskeleton organization, cell-cell adhesion, and extracellular matrix dynamics[72]. In endothelial cells, GATA4 acts as a regulator of chromatin accessibility[73].

In conclusion, we demonstrate that the epigenetic changes in the mouse kidney endothelium in response to endotoxemia are dependent on the expression of the IL-6 negative regulator SOCS3. In vitro, we show that IL-6 signaling directly promotes a sustained alteration in DNA methylation that may mediate many of the changes in endothelial gene expression. Our bioinformatic analysis suggest the potential involvement of specific transcription factors in the regulation of these epigenetic changes, providing potential candidate targets to limit the long-term damage induced by shock.

Legends to figures

Figure 1. Global analysis of DNA methylation in the endothelium after a single endotoxin challenge. (A) Severity score of mice 14 hours after saline or LPS injection. **(B)** Temperature for each mouse was measured immediately before and 14.5 hours post-injection. **(C)** Schematic of the experimental approach for isolating kidney endothelial cells. **(D)** Expression of the epithelial marker E-cadherin (CDH1) and the endothelial marker Von Willebrand factor (VWF) in endothelial-specific (after pulldown) vs. total (before pulldown) RNA from the same organ. **(E)** Volcano plot of differentially methylated positions CpG sites showing the p-value vs. Δβ for control and LPS-treated mice. **(F)** Gene ontology analysis of genes associated with differentially methylated CpG sites showing the most relevant enriched categories (blue mark for the hypermethylated set, and red mark for the hypomethylated set). **(G)** Box plots showing β values obtained from the DNA methylation array (all $p < 0.05$). We observed hypermethylation and hypomethylation in inflammatory response genes and cell regulation. Asterisks in A, B, and E denote $p < 0.05$, Student's t test.

Figure 2. Loss of endothelial SOCS3 promotes changes of DNA methylation in the endothelium. (A) RT-qPCR of enriched endothelial cells showing the increased levels of IL6 expression in $SOCS3^{iEKO}$ mice after LPS treatment. Mean ± SE fold-change expressed vs WT control mice. Asterisks denote $p < 0.05$, Student's t test. **(B)** Volcano plot of differentially methylated positions CpG sites showing the p-value vs. Δβ for LPS-treated WT and $SOCS3^{iEKO}$ (KO) mice. **(C)** Gene ontology analysis of genes associated with differentially methylated CpG sites showing the most relevant enriched categories (blue mark for the hypermethylated set, and red mark for the hypomethylated set). **(D)** Box plots showing β-values obtained from the DNA methylation array (all $p < 0.05$). **(E)** TF binding motif analysis of differentially methylated positions between LPS-treated WT and $SOCS3^{iEKO}$ mice. The panel shows TF family, TF member, and p-value of enrichment. Motif consensus is representative of the TF family.

Figure 3. Sustained treatment with IL-6+R induced DNA methylation changes in HUVEC. (A) Gene expression measured by RT-qPCR of HUVEC treated or not with IL-6+R for 72 hours. Mean ± SE fold change expressed vs. PBS-treated cells. Asterisks denote $p < 0.05$, Student's t test. **(B)** DNA methylation heatmap showing differentially methylated CpG sites between cells treated or not for 72 hours with IL-6+R. The heatmap includes all CpG-containing probes that display significant methylation changes ($p < 0.01$ and false discovery rate (FDR) < 0.05). **(C)** Barplot representing the percentages of different genomic features of hypomethylated (left panel) and hypermethylated (right panel) positions. **(D)** Gene ontology analysis of genes associated with differentially methylated CpG sites showing the most relevant enriched categories (blue mark for the hypermethylated set, and red mark for the hypomethylated set). **(E)** Correlation between DNA methylation changes and mRNA expression of candidate genes 72 hours post IL-6+R treatment. Data compiled from at least three independent experiments.

Figure 4. IL-6+R induced persistent gene expression changes. (A) Levels of IL6 mRNA as measured by RT-qPCR obtained from HUVEC cells, showing increased levels 72 hours post-IL-6+R treatment (0 h after wash), and its decrease after treatment washout. Mean ± SE fold-change expressed vs. PBS-treated cells. Asterisks denote $p < 0.05$ (One-way ANOVA). **(B)** Representative Western blot analysis of duplicate samples per treatment showing an increased level of STAT3 phosphorylation at tyrosine 705 post-IL-6+R treatment and a decrease to baseline levels 24 or 96 hours after cytokine washout (PBS was used as vehicle control). **(C)** mRNA expression of LAMP3 comparing cells treated with or without IL-6+R for 72 h and then incubated for additional 96 h in the absence of IL-6+R. Mean ± SE fold-change expressed vs. PBS-treated cells. Asterisk denotes $p < 0.05$, Student's t test. **A-C**, all data is representative of three independent experiments.

Figure 5. IL-6+R induced persistent DNA methylation. (A) Schematic diagram depicting in vitro experiments for IL-6+R washout (left) and DNA methylation heatmap showing differentially methylated CpGs that are retained after IL-6 washout (right). The heatmap includes all CpG-containing probes after 96 hours wash displaying a mean difference of less than 2% in methylation compared to IL-6+R for 72 hours. **(B)** TF binding motif analysis of differentially methylated CpGs between IL-6+R for 72 hours and 96 hours wash. The panel shows TF family, TF member, and p-value of enrichment. Motif consensus is representative of the TF family. Data from three independent experiments.

References

[1] van der Slikke EC, An AY, Hancock REW, Bouma HR: Exploring the pathophysiology of post-sepsis syndrome to identify therapeutic opportunities. EBioMedicine 2020, 61:103044.
[2] Peng Z, Shu B, Zhang Y, Wang M: Endothelial Response to Pathophysiological Stress. Arterioscler Thromb Vasc Biol 2019, 39:e233-e43.
[3] Ince C, Mayeux PR, Nguyen T, Gomez H, Kellum JA, Ospina-Tascon GA, Hernandez G, Murray P, De Backer D, Workgroup AX: The Endothelium in Sepsis. Shock 2016, 45:259-70.
[4] Mikkelsen ME, Still M, Anderson BJ, Bienvenu OJ, Brodsky MB, Brummel N, Butcher B, Clay AS, Felt H, Ferrante LE, Haines KJ, Harhay MO, Hope AA, Hopkins RO, Hosey M, Hough CTL, Jackson JC, Johnson A, Khan B, Lone NI, MacTavish P, McPeake J, Montgomery-Yates A, Needham DM, Netzer G, Schorr C, Skidmore B, Stollings JL, Umberger R, Andrews A, Iwashyna TJ, Sevin CM: Society of Critical Care Medicine's International Consensus Conference on Prediction and Identification of Long-Term Impairments After Critical Illness. Critical care medicine 2020, 48:1670-9.
[5] Binnie A, Walsh CJ, Hu P, Dwivedi DJ, Fox-Robichaud A, Liaw PC, Tsang JLY, Batt J, Carrasqueiro G, Gupta S, Marshall JC, Castelo-Branco P, Dos Santos CC, Epigenetic Profiling in Severe Sepsis Study of the Canadian Critical Care Translational Biology G: Epigenetic Profiling in Severe Sepsis: A Pilot Study of DNA Methylation Profiles in Critical Illness. Crit Care Med 2020, 48:142-50.
[6] Hopp L, Loeffler-Wirth H, Nersisyan L, Arakelyan A, Binder H: Footprints of Sepsis Framed Within Community Acquired Pneumonia in the Blood Transcriptome. Front Immunol 2018, 9:1620.
[7] Cao L, Zhu T, Lang X, Jia S, Yang Y, Zhu C, Wang Y, Feng S, Wang C, Zhang P, Chen J, Jiang H: Inhibiting DNA Methylation Improves Survival in Severe Sepsis by Regulating NF-kappaB Pathway. Front Immunol 2020, 11:1360.
[8] Falcao-Holanda RB, Brunialti MKC, Jasiulionis MG, Salomao R: Epigenetic Regulation in Sepsis, Role in Pathophysiology and Therapeutic Perspective. Front Med (Lausanne) 2021, 8:685333.
[9] Cross D, Drury R, Hill J, Pollard AJ: Epigenetics in Sepsis: Understanding Its Role in Endothelial Dysfunction, Immunosuppression, and Potential Therapeutics. Front Immunol 2019, 10:1363.
[10] Hunter CA, Jones SA: IL-6 as a keystone cytokine in health and disease. Nature immunology 2015, 16:448-57.
[11] Hirano T: Interleukin 6 in autoimmune and inflammatory diseases: a personal memoir. Proceedings of the Japan Academy Series B, Physical and biological sciences 2010, 86:717-30.
[12] Takahashi W, Nakada TA, Yazaki M, Oda S: Interleukin-6 Levels Act as a Diagnostic Marker for Infection and a Prognostic Marker in Patients with Organ Dysfunction in Intensive Care Units. Shock 2016, 46:254-60.
[13] Kang S, Kishimoto T: Interplay between interleukin-6 signaling and the vascular endothelium in cytokine storms. Exp Mol Med 2021, 53:1116-23.
[14] Villarino AV, Kanno Y, O'Shea JJ: Mechanisms and consequences of Jak-STAT signaling in the immune system. Nat Immunol 2017, 18:374-84.

[15] Babon JJ, Varghese LN, Nicola NA: Inhibition of IL-6 family cytokines by SOCS3. Semin Immunol 2014, 26:13-9.
[16] Alsaffar H, Martino N, Garrett JP, Adam AP: Interleukin-6 promotes a sustained loss of endothelial barrier function via Janus kinase-mediated STAT3 phosphorylation and de novo protein synthesis. American journal of physiology Cell physiology 2018, 314:C589-C602.
[17] Martino N, Bossardi Ramos R, Chuy D, Tomaszek L, Adam AP: SOCS3 limits TNF and endotoxin-induced endothelial dysfunction by blocking a required autocrine interleukin 6 signal in human endothelial cells. American journal of physiology Cell physiology 2022.
[18] Martino N, Ramos RB, Lu S, Leyden K, Tomaszek L, Sadhu S, Fredman G, Jaitovich A, Vincent PA, Adam AP: Endothelial SOCS3 maintains homeostasis and promotes survival in endotoxemic mice. JCI Insight 2021, 6.
[19] Wang Y, Nakayama M, Pitulescu ME, Schmidt TS, Bochenek ML, Sakakibara A, Adams S, Davy A, Deutsch U, Luthi U, Barberis A, Benjamin LE, Makinen T, Nobes CD, Adams RH: Ephrin-B2 controls VEGF-induced angiogenesis and lymphangiogenesis. Nature 2010, 465:483-6.
[20] Madisen L, Zwingman TA, Sunkin SM, Oh SW, Zariwala HA, Gu H, Ng LL, Palmiter RD, Hawrylycz MJ, Jones AR, Lein ES, Zeng H: A robust and high-throughput Cre reporting and characterization system for the whole mouse brain. Nature neuroscience 2010, 13:133-40.
[21] Yasukawa H, Ohishi M, Mori H, Murakami M, Chinen T, Aki D, Hanada T, Takeda K, Akira S, Hoshijima M, Hirano T, Chien KR, Yoshimura A: IL-6 induces an anti-inflammatory response in the absence of SOCS3 in macrophages. Nature immunology 2003, 4:551-6.
[22] Valle ML, Dworshak J, Sharma A, Ibrahim AS, Al-Shabrawey M, Sharma S: Inhibition of interleukin-6 trans-signaling prevents inflammation and endothelial barrier disruption in retinal endothelial cells. Experimental eye research 2019, 178:27-36.
[23] Gimbrone MA, Jr., Cotran RS, Folkman J: Human vascular endothelial cells in culture. Growth and DNA synthesis. The Journal of cell biology 1974, 60:673-84.
[24] Jaffe EA, Nachman RL, Becker CG, Minick CR: Culture of human endothelial cells derived from umbilical veins. Identification by morphologic and immunologic criteria. The Journal of clinical investigation 1973, 52:2745-56.
[25] Bibikova M, Barnes B, Tsan C, Ho V, Klotzle B, Le JM, Delano D, Zhang L, Schroth GP, Gunderson KL, Fan JB, Shen R: High density DNA methylation array with single CpG site resolution. Genomics 2011, 98:288-95.
[26] Morris TJ, Butcher LM, Feber A, Teschendorff AE, Chakravarthy AR, Wojdacz TK, Beck S: ChAMP: 450k Chip Analysis Methylation Pipeline. Bioinformatics 2014, 30:428-30.
[27] Aryee MJ, Jaffe AE, Corrada-Bravo H, Ladd-Acosta C, Feinberg AP, Hansen KD, Irizarry RA: Minfi: a flexible and comprehensive Bioconductor package for the analysis of Infinium DNA methylation microarrays. Bioinformatics 2014, 30:1363-9.
[28] Fortin JP, Triche TJ, Jr., Hansen KD: Preprocessing, normalization and integration of the Illumina HumanMethylationEPIC array with minfi. Bioinformatics 2017, 33:558-60.
[29] Teschendorff AE, Marabita F, Lechner M, Bartlett T, Tegner J, Gomez-Cabrero D, Beck S: A beta-mixture quantile normalization method for correcting probe design bias in Illumina Infinium 450 k DNA methylation data. Bioinformatics 2013, 29:189-96.
[30] Assenov Y, Muller F, Lutsik P, Walter J, Lengauer T, Bock C: Comprehensive analysis of DNA methylation data with RnBeads. Nat Methods 2014, 11:1138-40.
[31] Chen YA, Lemire M, Choufani S, Butcher DT, Grafodatskaya D, Zanke BW, Gallinger S, Hudson TJ, Weksberg R: Discovery of cross-reactive probes and polymorphic CpGs in the Illumina Infinium HumanMethylation450 microarray. Epigenetics 2013, 8:203-9.
[32] Triche TJ, Jr., Weisenberger DJ, Van Den Berg D, Laird PW, Siegmund KD: Low-level processing of Illumina Infinium DNA Methylation BeadArrays. Nucleic Acids Res 2013, 41:e90.

[33] Du P, Zhang X, Huang CC, Jafari N, Kibbe WA, Hou L, Lin SM: Comparison of Beta-value and M-value methods for quantifying methylation levels by microarray analysis. BMC Bioinformatics 2010, 11:587.
[34] Zhou Y, Zhou B, Pache L, Chang M, Khodabakhshi AH, Tanaseichuk O, Benner C, Chanda SK: Metascape provides a biologist-oriented resource for the analysis of systems-level datasets. Nature communications 2019, 10:1523.
[35] Heinz S, Benner C, Spann N, Bertolino E, Lin YC, Laslo P, Cheng JX, Murre C, Singh H, Glass CK: Simple combinations of lineage-determining transcription factors prime cis-regulatory elements required for macrophage and B cell identities. Molecular cell 2010, 38:576-89.
[36] Ziller MJ, Gu H, Muller F, Donaghey J, Tsai LT, Kohlbacher O, De Jager PL, Rosen ED, Bennett DA, Bernstein BE, Gnirke A, Meissner A: Charting a dynamic DNA methylation landscape of the human genome. Nature 2013, 500:477-81.
[37] Guo C, Dong G, Liang X, Dong Z: Epigenetic regulation in AKI and kidney repair: mechanisms and therapeutic implications. Nature reviews Nephrology 2019, 15:220-39.
[38] Wu Q, Maniatis T: A striking organization of a large family of human neural cadherin-like cell adhesion genes. Cell 1999, 97:779-90.
[39] Tsutsui K, Manabe R, Yamada T, Nakano I, Oguri Y, Keene DR, Sengle G, Sakai LY, Sekiguchi K: ADAMTSL-6 is a novel extracellular matrix protein that binds to fibrillin-1 and promotes fibrillin-1 fibril formation. J Biol Chem 2010, 285:4870-82.
[40] Petit MM, Fradelizi J, Golsteyn RM, Ayoubi TA, Menichi B, Louvard D, Van de Ven WJ, Friederich E: LPP, an actin cytoskeleton protein related to zyxin, harbors a nuclear export signal and transcriptional activation capacity. Mol Biol Cell 2000, 11:117-29.
[41] Malinin NL, Boldin MP, Kovalenko AV, Wallach D: MAP3K-related kinase involved in NF-kappaB induction by TNF, CD95 and IL-1. Nature 1997, 385:540-4.
[42] Ortiz A, Husi H, Gonzalez-Lafuente L, Valino-Rivas L, Fresno M, Sanz AB, Mullen W, Albalat A, Mezzano S, Vlahou T, Mischak H, Sanchez-Nino MD: Mitogen-Activated Protein Kinase 14 Promotes AKI. J Am Soc Nephrol 2017, 28:823-36.
[43] Kim EC, Edmonston CR, Wu X, Schaffer A, Casali P: The HoxC4 homeodomain protein mediates activation of the immunoglobulin heavy chain 3' hs1,2 enhancer in human B cells. Relevance to class switch DNA recombination. J Biol Chem 2004, 279:42258-69.
[44] Zeng J, Sun W, Chang J, Yi D, Zhu L, Zhang Y, Pan X, Zhou Y, Lai M, Bian G, Zhou Q, Liu J, Chen B, Ma F: HOXC4 up-regulates NF-kappaB signaling and promotes the cell proliferation to drive development of human hematopoiesis, especially CD43+ cells. Blood Sci 2020, 2:117-28.
[45] Liu ZH, Li C, Chen JW, Shen Y, Gao J, Shen WF, Zhang RY, Wang XQ, Lu L: C1q/TNF-related protein 1 promotes endothelial barrier dysfunction under disturbed flow. Biochem Biophys Res Commun 2017, 490:580-6.
[46] Albright RA, Chang WC, Robert D, Ornstein DL, Cao W, Liu L, Redick ME, Young JI, De La Cruz EM, Braddock DT: NPP4 is a procoagulant enzyme on the surface of vascular endothelium. Blood 2012, 120:4432-40.
[47] Burton TD, Fedele AO, Xie J, Sandeman LY, Proud CG: The gene for the lysosomal protein LAMP3 is a direct target of the transcription factor ATF4. J Biol Chem 2020, 295:7418-30.
[48] Kroon J, Schaefer A, van Rijssel J, Hoogenboezem M, van Alphen F, Hordijk P, Stroes ESG, Stromblad S, van Rheenen J, van Buul JD: Inflammation-Sensitive Myosin-X Functionally Supports Leukocyte Extravasation by Cdc42-Mediated ICAM-1-Rich Endothelial Filopodia Formation. J Immunol 2018, 200:1790-801.
[49] Melenhorst WB, van den Heuvel MC, Timmer A, Huitema S, Bulthuis M, Timens W, van Goor H: ADAM19 expression in human nephrogenesis and renal disease: associations with clinical and structural deterioration. Kidney Int 2006, 70:1269-78.
[50] Meder B, Haas J, Sedaghat-Hamedani F, Kayvanpour E, Frese K, Lai A, Nietsch R, Scheiner C, Mester S, Bordalo DM, Amr A, Dietrich C, Pils D, Siede D, Hund H, Bauer A, Holzer

DB, Ruhparwar A, Mueller-Hennessen M, Weichenhan D, Plass C, Weis T, Backs J, Wuerstle M, Keller A, Katus HA, Posch AE: Epigenome-Wide Association Study Identifies Cardiac Gene Patterning and a Novel Class of Biomarkers for Heart Failure. Circulation 2017, 136:1528-44.
[51] Pepin ME, Ha CM, Crossman DK, Litovsky SH, Varambally S, Barchue JP, Pamboukian SV, Diakos NA, Drakos SG, Pogwizd SM, Wende AR: Genome-wide DNA methylation encodes cardiac transcriptional reprogramming in human ischemic heart failure. Lab Invest 2019, 99:371-86.
[52] Glezeva N, Moran B, Collier P, Moravec CS, Phelan D, Donnellan E, Russell-Hallinan A, O'Connor DP, Gallagher WM, Gallagher J, McDonald K, Ledwidge M, Baugh J, Das S, Watson CJ: Targeted DNA Methylation Profiling of Human Cardiac Tissue Reveals Novel Epigenetic Traits and Gene Deregulation Across Different Heart Failure Patient Subtypes. Circ Heart Fail 2019, 12:e005765.
[53] Russell-Hallinan A, Watson CJ, O'Dwyer D, Grieve DJ, O'Neill KM: Epigenetic Regulation of Endothelial Cell Function by Nucleic Acid Methylation in Cardiac Homeostasis and Disease. Cardiovasc Drugs Ther 2021, 35:1025-44.
[54] Giannitsi S, Bougiakli M, Bechlioulis A, Naka K: Endothelial dysfunction and heart failure: A review of the existing bibliography with emphasis on flow mediated dilation. JRSM Cardiovasc Dis 2019, 8:2048004019843047.
[55] Novakovic B, Habibi E, Wang SY, Arts RJW, Davar R, Megchelenbrink W, Kim B, Kuznetsova T, Kox M, Zwaag J, Matarese F, van Heeringen SJ, Janssen-Megens EM, Sharifi N, Wang C, Keramati F, Schoonenberg V, Flicek P, Clarke L, Pickkers P, Heath S, Gut I, Netea MG, Martens JHA, Logie C, Stunnenberg HG: beta-Glucan Reverses the Epigenetic State of LPS-Induced Immunological Tolerance. Cell 2016, 167:1354-68 e14.
[56] El Gazzar M, Yoza BK, Chen X, Hu J, Hawkins GA, McCall CE: G9a and HP1 couple histone and DNA methylation to TNFalpha transcription silencing during endotoxin tolerance. J Biol Chem 2008, 283:32198-208.
[57] Zhao Y, Ding C, Xue W, Ding X, Zheng J, Gao Y, Xia X, Li S, Liu J, Han F, Zhu F, Tian P: Genome-wide DNA methylation analysis in renal ischemia reperfusion injury. Gene 2017, 610:32-43.
[58] Zhang XQ, Lv CJ, Liu XY, Hao D, Qin J, Tian HH, Li Y, Wang XZ: Genomewide analysis of DNA methylation in rat lungs with lipopolysaccharideinduced acute lung injury. Mol Med Rep 2013, 7:1417-24.
[59] Binnie A, Tsang JLY, Hu P, Carrasqueiro G, Castelo-Branco P, Dos Santos CC: Epigenetics of Sepsis. Crit Care Med 2020, 48:745-56.
[60] Feletou M, Vanhoutte PM: Endothelial dysfunction: a multifaceted disorder. Am J Physiol-Heart Circul Physiol 2006, 291:H985-H1002.
[61] van Ierssel SH, Jorens PG, Van Craenenbroeck EM, Conraads VM: The Endothelium, A Protagonist in the Pathophysiology of Critical Illness: Focus on Cellular Markers. Biomed Research International 2014, 2014:10.
[62] Endemann DH, Schiffrin EL: Endothelial dysfunction. J Am Soc Nephrol 2004, 15:1983-92.
[63] Coletta C, Módis K, Oláh G, Brunyánszki A, Herzig DS, Sherwood ER, Ungvári Z, Szabo C: Endothelial dysfunction is a potential contributor to multiple organ failure and mortality in aged mice subjected to septic shock: preclinical studies in a murine model of cecal ligation and puncture. Critical Care 2014, 18:511.
[64] Chang JC: Sepsis and septic shock: endothelial molecular pathogenesis associated with vascular microthrombotic disease. Thrombosis Journal 2019, 17:10.
[65] Bossardi Ramos R, Adam AP: Molecular Mechanisms of Vascular Damage During Lung Injury. Advances in experimental medicine and biology 2021, 1304:95-107.
[66] Iskander KN, Craciun FL, Stepien DM, Duffy ER, Kim J, Moitra R, Vaickus LJ, Osuchowski MF, Remick DG: Cecal ligation and puncture-induced murine sepsis does not cause lung injury. Critical care medicine 2013, 41:159-70.

[67] Jeong HW, Hernandez-Rodriguez B, Kim J, Kim KP, Enriquez-Gasca R, Yoon J, Adams S, Scholer HR, Vaquerizas JM, Adams RH: Transcriptional regulation of endothelial cell behavior during sprouting angiogenesis. Nature communications 2017, 8:726.
[68] Lorente-Sorolla C, Garcia-Gomez A, Catala-Moll F, Toledano V, Ciudad L, Avendano-Ortiz J, Maroun-Eid C, Martin-Quiros A, Martinez-Gallo M, Ruiz-Sanmartin A, Del Campo AG, Ferrer-Roca R, Ruiz-Rodriguez JC, Alvarez-Errico D, Lopez-Collazo E, Ballestar E: Inflammatory cytokines and organ dysfunction associate with the aberrant DNA methylome of monocytes in sepsis. Genome Med 2019, 11:66.
[69] Morante-Palacios O, Lorente-Sorolla C, Ciudad L, Calafell-Segura J, Garcia-Gomez A, Catala-Moll F, Ruiz-Sanmartin A, Martinez-Gallo M, Ferrer R, Ruiz-Rodriguez JC, Alvarez-Errico D, Ballestar E: JAK2-STAT Epigenetically Regulates Tolerized Genes in Monocytes in the First Encounter With Gram-Negative Bacterial Endotoxins in Sepsis. Front Immunol 2021, 12:734652.
[70] Yang Y, Cvekl A: Large Maf Transcription Factors: Cousins of AP-1 Proteins and Important Regulators of Cellular Differentiation. Einstein J Biol Med 2007, 23:2-11.
[71] Dieterich LC, Klein S, Mathelier A, Sliwa-Primorac A, Ma Q, Hong YK, Shin JW, Hamada M, Lizio M, Itoh M, Kawaji H, Lassmann T, Daub CO, Arner E, Carninci P, Hayashizaki Y, Forrest ARR, Wasserman WW, Detmar M: DeepCAGE Transcriptomics Reveal an Important Role of the Transcription Factor MAFB in the Lymphatic Endothelium. Cell Rep 2015, 13:1493-504.
[72] Soini T, Eloranta K, Pihlajoki M, Kyronlahti A, Akinrinade O, Andersson N, Lohi J, Pakarinen MP, Wilson DB, Heikinheimo M: Transcription factor GATA4 associates with mesenchymal-like gene expression in human hepatoblastoma cells. Tumour Biol 2018, 40:1010428318785498.
[73] Winkler M, Staniczek T, Kurschner SW, Schmid CD, Schonhaber H, Cordero J, Kessler L, Mathes A, Sticht C, Nessling M, Uvarovskii A, Anders S, Zhang XJ, von Figura G, Hartmann D, Mogler C, Dobreva G, Schledzewski K, Geraud C, Koch PS, Goerdt S: Endothelial GATA4 controls liver fibrosis and regeneration by preventing a pathogenic switch in angiocrine signaling. J Hepatol 2021, 74:380-93.

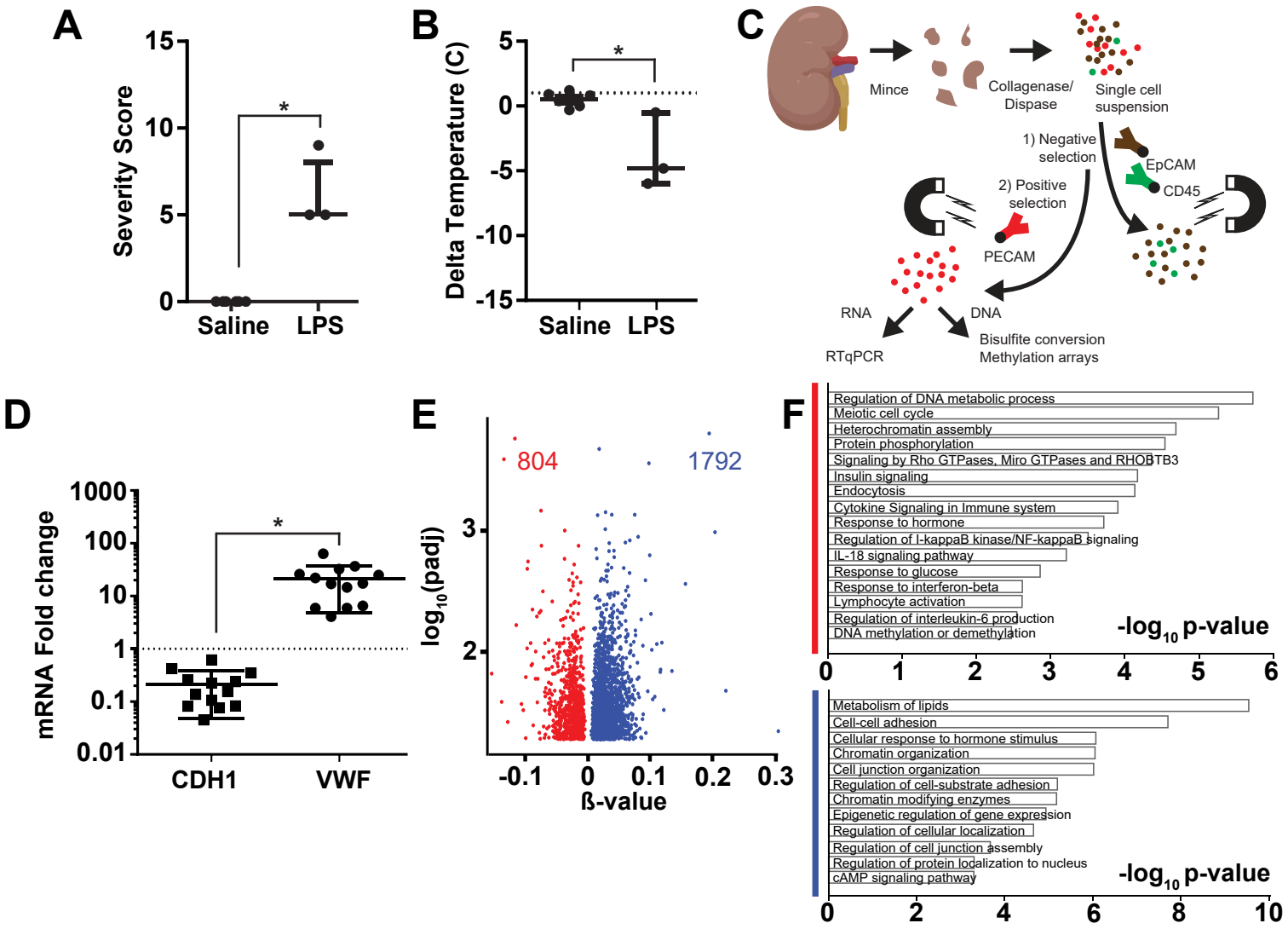
A
Severity Score
15
10
5
0
*
Saline
LPS
B
Delta Temperature (C)
5
0
-5
-10
-15
*
Saline
LPS
C
Mince
Collagenase/
Dispase
Single cell
suspension
1) Negative
selection
EpCAM
CD45
2) Positive
selection
PECAM
RNA
DNA
RTqPCR
Bisulfite conversion
Methylation arrays
D
mRNA Fold change
1000
100
10
1
0.1
0.01
*
CDH1
VWF
E
804
1792
log10(padj)
3
2
-0.1
0
0.1
0.2
0.3
ß-value
F
Regulation of DNA metabolic process
Meiotic cell cycle
Heterochromatin assembly
Protein phosphorylation
Signaling by Rho GTPases, Miro GTPases and RHOBTB3
Insulin signaling
Endocytosis
Cytokine Signaling in Immune system
Response to hormone
Regulation of I-kappaB kinase/NF-kappaB signaling
IL-18 signaling pathway
Response to glucose
Response to interferon-beta
Lymphocyte activation
Regulation of interleukin-6 production
DNA methylation or demethylation
-log10 p-value
0
1
2
3
4
5
6
Metabolism of lipids
Cell-cell adhesion
Cellular response to hormone stimulus
Chromatin organization
Cell junction organization
Regulation of cell-substrate adhesion
Chromatin modifying enzymes
Epigenetic regulation of gene expression
Regulation of cellular localization
Regulation of cell junction assembly
Regulation of protein localization to nucleus
cAMP signaling pathway
-log10 p-value
0
2
4
6
8
10
G
LPP
cg46825966
MAP3K14
cg30076769
Pcdha1
cg35608636
Thsd4
cg46825966
ß-value
0.8
0.7
0.6
0.5
0.4
0.3
Saline
LPS

Figure 1

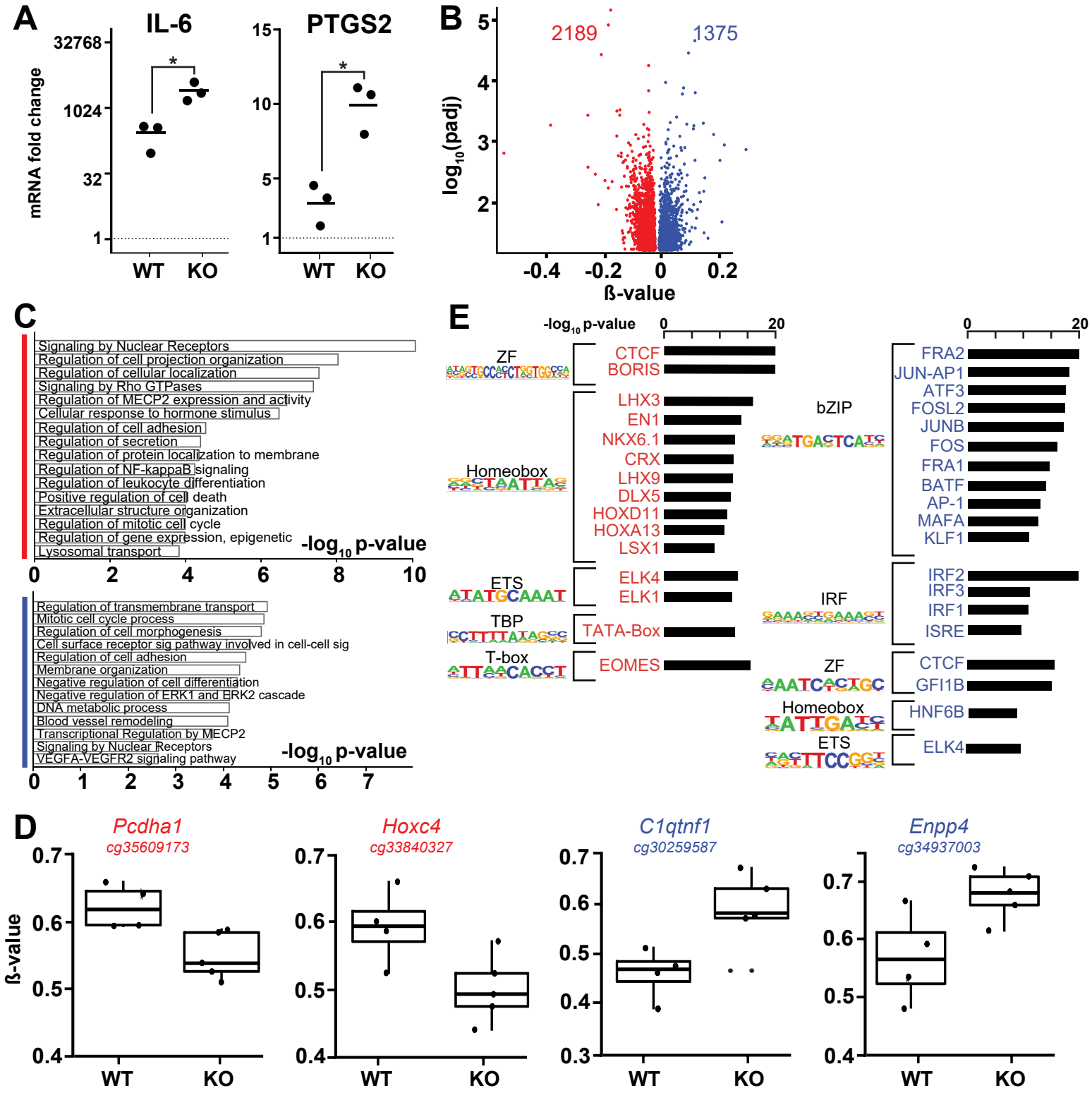
A
IL-6
PTGS2
mRNA fold change
32768
1024
32
1
15
10
5
1
*
*
WT
KO
WT
KO
B
2189
1375
log10(padj)
5
4
3
2
-0.4
-0.2
0
0.2
ß-value
C
Signaling by Nuclear Receptors
Regulation of cell projection organization
Regulation of cellular localization
Signaling by Rho GTPases
Regulation of MECP2 expression and activity
Cellular response to hormone stimulus
Regulation of cell adhesion
Regulation of secretion
Regulation of protein localization to membrane
Regulation of NF-kappaB signaling
Regulation of leukocyte differentiation
Positive regulation of cell death
Extracellular structure organization
Regulation of mitotic cell cycle
Regulation of gene expression, epigenetic
Lysosomal transport
-log10 p-value
0
2
4
6
8
10
Regulation of transmembrane transport
Mitotic cell cycle process
Regulation of cell morphogenesis
Cell surface receptor sig pathway involved in cell-cell sig
Regulation of cell adhesion
Membrane organization
Negative regulation of cell differentiation
Negative regulation of ERK1 and ERK2 cascade
DNA metabolic process
Blood vessel remodeling
Transcriptional Regulation by MECP2
Signaling by Nuclear Receptors
VEGFA-VEGFR2 signaling pathway
-log10 p-value
0
1
2
3
4
5
6
7
E
-log10 p-value
0
20
ZF
CTCF
BORIS
Homeobox
LHX3
EN1
NKX6.1
CRX
LHX9
DLX5
HOXD11
HOXA13
LSX1
ETS
ATATGCAAAT
ELK4
ELK1
TBP
TATA-Box
T-box
EOMES
bZIP
FRA2
JUN-AP1
ATF3
FOSL2
JUNB
FOS
FRA1
BATF
AP-1
MAFA
KLF1
IRF
IRF2
IRF3
IRF1
ISRE
ZF
CTCF
GFI1B
Homeobox
HNF6B
ETS
ELK4
D
Pcdha1
cg35609173
Hoxc4
cg33840327
C1qtnf1
cg30259587
Enpp4
cg34937003
ß-value
0.7
0.6
0.5
0.4
0.3
WT
KO

Figure 2

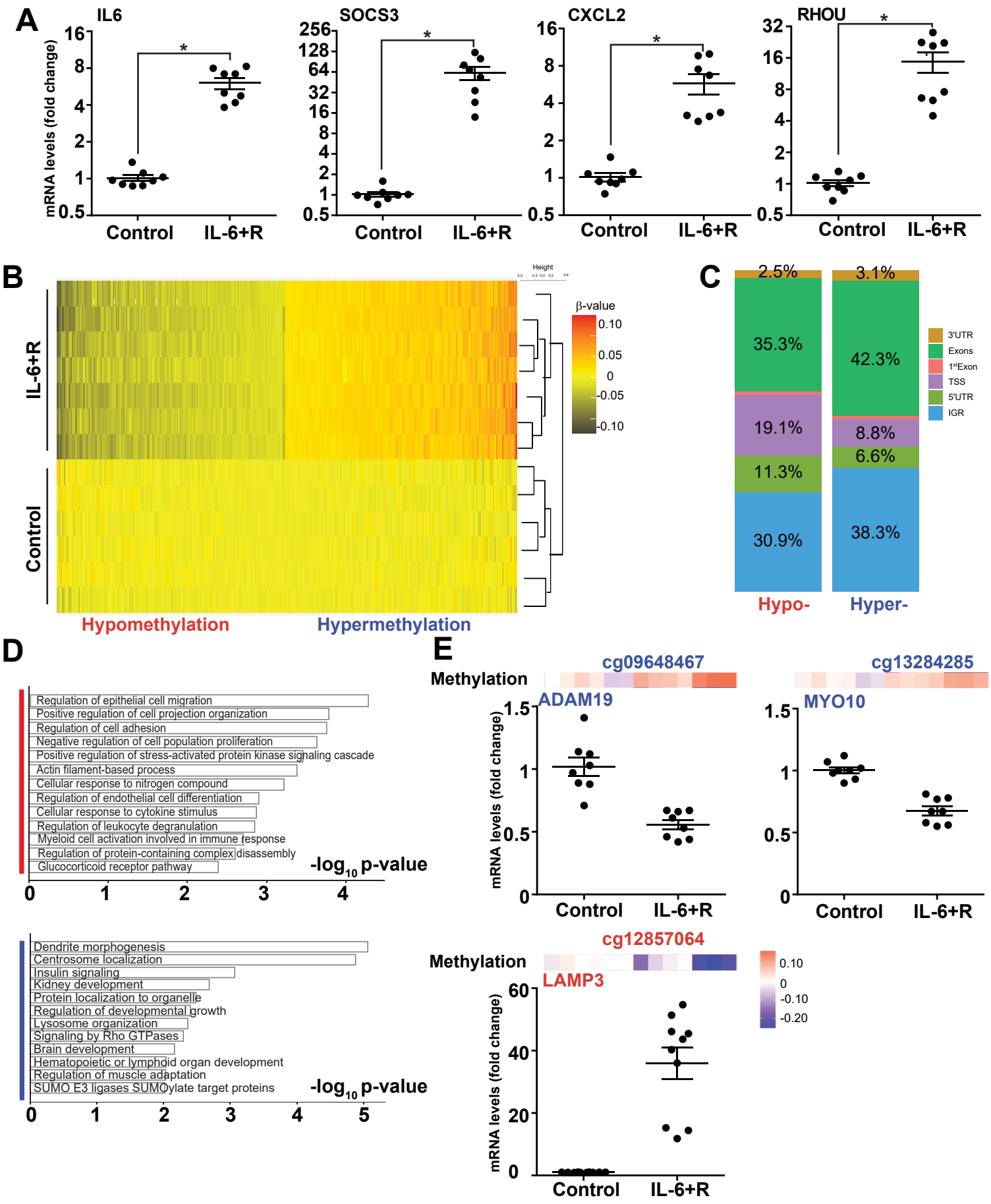
A
IL6
SOCS3
CXCL2
RHOU
mRNA levels (fold change)
Control
IL-6+R
B
Height
β-value
0.10
0.05
0
-0.05
-0.10
IL-6+R
Control
Hypomethylation
Hypermethylation
C
2.5%
3.1%
35.3%
42.3%
19.1%
8.8%
6.6%
11.3%
30.9%
38.3%
3'UTR
Exons
1stExon
TSS
5'UTR
IGR
Hypo-
Hyper-
D
Regulation of epithelial cell migration
Positive regulation of cell projection organization
Regulation of cell adhesion
Negative regulation of cell population proliferation
Positive regulation of stress-activated protein kinase signaling cascade
Actin filament-based process
Cellular response to nitrogen compound
Regulation of endothelial cell differentiation
Cellular response to cytokine stimulus
Regulation of leukocyte degranulation
Myeloid cell activation involved in immune response
Regulation of protein-containing complex disassembly
Glucocorticoid receptor pathway
-log10 p-value
Dendrite morphogenesis
Centrosome localization
Insulin signaling
Kidney development
Protein localization to organelle
Regulation of developmental growth
Lysosome organization
Signaling by Rho GTPases
Brain development
Hematopoietic or lymphoid organ development
Regulation of muscle adaptation
SUMO E3 ligases SUMOylate target proteins
-log10 p-value
E
Methylation
cg09648467
ADAM19
cg13284285
MYO10
cg12857064
LAMP3
mRNA levels (fold change)
Control
IL-6+R
0.10
0
-0.10
-0.20

Figure 3

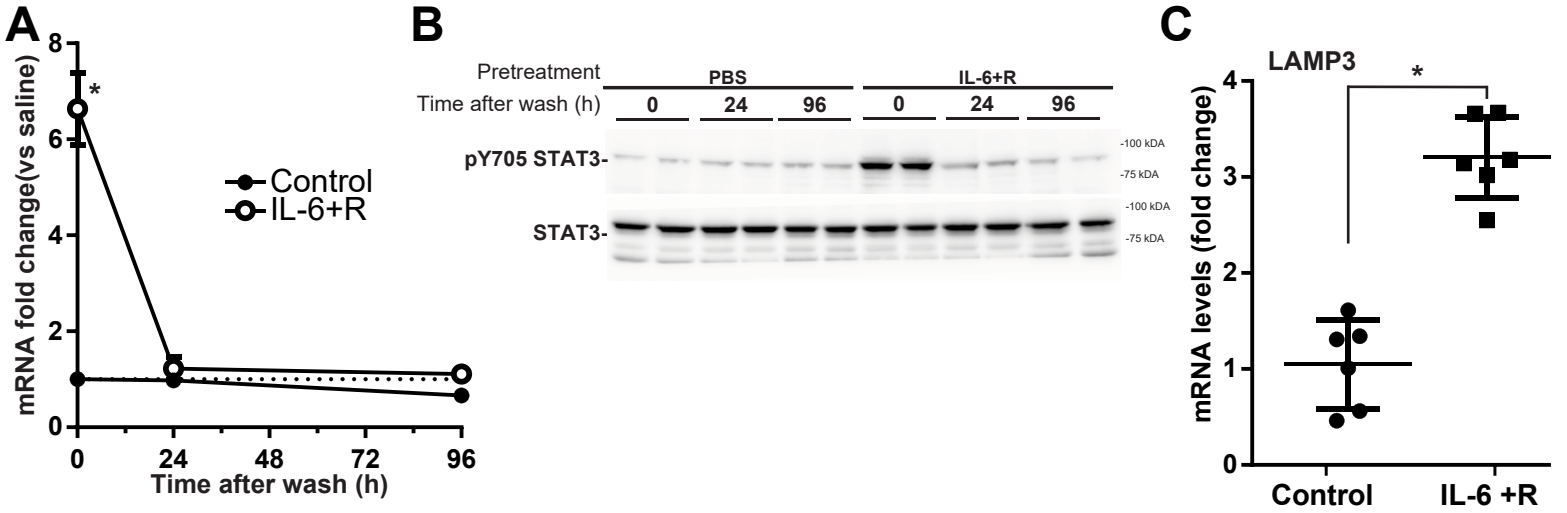
A
mRNA fold change(vs saline)
Time after wash (h)
Control
IL-6+R
*
B
Pretreatment
PBS
IL-6+R
Time after wash (h)
0
24
96
0
24
96
pY705 STAT3-
STAT3-
-100 kDA
-75 kDA
C
LAMP3
mRNA levels (fold change)
Control
IL-6 +R
*

Figure 4

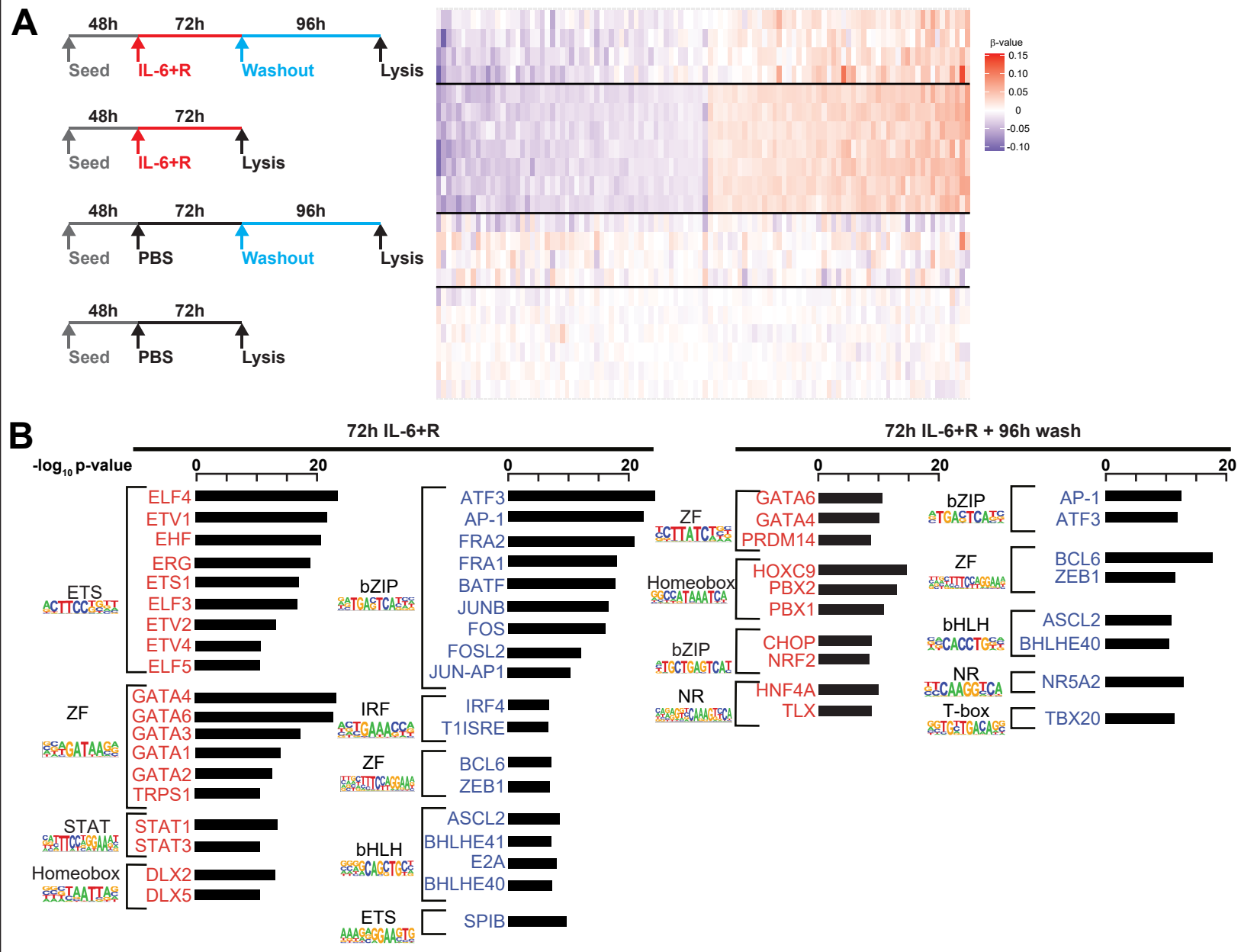
A
48h
72h
96h
Seed
IL-6+R
Washout
Lysis
48h
72h
Seed
IL-6+R
Lysis
48h
72h
96h
Seed
PBS
Washout
Lysis
48h
72h
Seed
PBS
Lysis
β-value
0.15
0.10
0.05
0
-0.05
-0.10
B
72h IL-6+R
72h IL-6+R + 96h wash
-log10 p-value
0
20
ETS
ELF4
ETV1
EHF
ERG
ETS1
ELF3
ETV2
ETV4
ELF5
ZF
GATA4
GATA6
GATA3
GATA1
GATA2
TRPS1
STAT
STAT1
STAT3
Homeobox
DLX2
DLX5
bZIP
ATF3
AP-1
FRA2
FRA1
BATF
JUNB
FOS
FOSL2
JUN-AP1
IRF
IRF4
T1ISRE
ZF
BCL6
ZEB1
bHLH
ASCL2
BHLHE41
E2A
BHLHE40
ETS
SPIB
ZF
GATA6
GATA4
PRDM14
Homeobox
HOXC9
PBX2
PBX1
bZIP
CHOP
NRF2
NR
HNF4A
TLX
bZIP
AP-1
ATF3
ZF
BCL6
ZEB1
bHLH
ASCL2
BHLHE40
NR
NR5A2
T-box
TBX20

Figure 5

Supplemental Table 1 - List of reagents and kits

M&M section	Reagent or disposable	Vendor	Catalog Number	Concentration
Mice	Tamoxifen	Sigma Aldrich	T5648	2 mg/100 µL
	Peanut Oil	Sigma Aldrich	P2144	N/A
	Lipopolysaccharide	Sigma Aldrich	L4391	250 µg/250µL
Endothelial Enrichment	Collagenase Type 1	Worthington Biochemicals	LS004196	0.2%
	Biotin anti-mouse CD326 (Ep-CAM) Antibody	Biolegend	118204	0.5 mg/mL
	Anti CD 31 Rat monoclonal Antibody	Biolegend	102504	0.5 mg/mL
	Biotinylated Anti Mouse CD45 Antibody	Biolegend	103104	0.5 mg/mL
	RNAse A	Sigma Aldrich	E866	100 mg/ml
	Dispase II	Roche	10295825001	0.2%
	Dneasy Blood and Tissue kit	Qiagen	69504	As per instructions
	RNEasy Plus Micro Kit	Qiagen	74034	As per instructions
	BD Falcon cell strainer 70um pore size	Thermo Fisher	352350	N/A
	Dynabeads M-280 Streptavidin	Thermo Scientific	11205D	1 mg/100 µL
Cell Culture	Trypsin-EDTA Solution 1X	Millipore Sigma	54917C-100ML	1X
	Recombinant Human IL6 protein	R&D Systems	206-IL-200/CF	200 ng/mL
	Recombinant human IL6r alpha, CF	R&D Systems	227-SR-025/CF	100 ng/mL
	phenol red-free EBM 2 media	PromoCell	C-22211	N/A
	Penicillin-Streptomycin Solution, 100x	Corning	30-002-CI-PK	1X
	Gelatin	Millipore Sigma	ES-006-B	0.1%

Gel Electrophoresis and Immunoblotting	Complete protease inhibitor mixture	Roche Applied Science	11697498001	1X
	PhosSTOP phosphatase inhibitor mixture	Roche Applied Science	4906845001	1X
	Sodium fluoride	Millipore Sigma	S-1504	100 mM
	Phenyl arsine oxide	Millipore Sigma	P-3075	100 μM
	Sodium pyrophosphate decahydrate	Millipore Sigma	221368-100G	10 mM
	Sodium orthovanadate	Millipore Sigma	S6508	100 μM
	Transblot Turbo RTA Mini Nitrocellulose - Transfer kit	Bio-Rad	1704270	N/A
	Clarity Western ECL Substrate	Bio-Rad	1705061	As per instructions
	Clarity Max Western ECL Substrate	Bio-Rad	1705062	As per instructions
RNA isolation and RTqPCR	PrimeScript RT Master Mix	Clontech	RR036B	1X
	TRIzol reagent	Invitrogen	15596018	1X
	iTaq Universal SYBR Green Supermix	Bio Rad	1725125	1X

Supplemental Table 2 - Sequence of PCR primers

Mouse qPCR primer sequences		
Primer name	**Forward Sequence**	**Reverse Sequence**
CDH1	GGTCATCAGTGTGCTCACCTCT	GCTGTTGTGCTCAAGCCTTCAC
VWF	AACAGACGATGGTGGACTCAGC	AACAGACGATGGTGGACTCAGC
PTGS2	GCGACATACTCAAGCAGGAGCA	AGTGGTAACCGCTCAGGTGTTG
IL-6	TACCACTTCACAAGTCGGAGGC	CTGCAAGTGCATCATCGTTGTTC
Human qPCR primer sequences		
IL-6	TACCACTTCACAAGTCGGAGGC	CTGCAAGTGCATCATCGTTGTTC
SOCS3	CATCTCTGTCGGAAGACCGTCA	GCATCGTACTGGTCCAGGAACT
CXCL2	GGCAGAAAGCTTGTCTCAACCC	CTCCTTCAGGAACAGCCACCAA
RHOU	ACTGCCTTCGACAACTTCTCCG	GAGCAGGAAGATGTCTGTGTTGG
ADAM19	CGAGAAGGTGAATGTGGCAGGA	AGCTCTGACACTGGATCTTCCC
MYO10	CACTCTGCCGTATTTCCACAGC	TTTGTGGAGCCAGCCTTGCTTG
LAMP3	TGGGAGCCTATTTGACCGTCTC	GCTGACAACTGGAGGCTCTGTT

Supplemental Table 3 - List of antibodies

Target	Species	Clone	Conjugate	Vendor	Catalog No	RRID	Dilution	Blocking solution
STAT3	rabbit	D1A5		Cell Signaling	8768S	AB_2722529	1:5000	5% BSA, 0.1% Tween 20 in PBS
pY705-STAT3	rabbit	D3A7		Cell Signaling	9145L	AB_2491009	1:5000	5% BSA, 0.1% Tween 20 in PBS
β-actin	mouse	AC-15		Millipore Sigma	A5441	AB_476744	1:10000	5% BSA, 0.1% Tween 20 in PBS
Mouse IgG (H+L)	goat	polyclonal	HRP	Jackson IR	115-035-062	AB_2338504	1:5000	5% BSA, 0.1% Tween 20 in PBS
Rabbit IgG (H+L)	rabbit	polyclonal	HRP	Jackson IR	111-035-003	AB_2313567	1:5000	5% BSA, 0.1% Tween 20 in PBS